Inhomogeneously broadening effect on temperature-dependent lineshape in single quantum dot luminescence

2008 J. Phys.: Condens. Matter 20 255244

(http://iopscience.iop.org/0953-8984/20/25/255244)

IOP Publishing Journal of Physics: Condensed Matter
J. Phys.: Condens. Matter **20** (2008) 255244 (6pp) doi:10.1088/0953-8984/20/25/255244

Inhomogeneously broadening effect on temperature-dependent lineshape in single quantum dot luminescence

W Q Li and J C Cao

State Key Laboratory of Functional Materials for Informatics, Shanghai Institute of Microsystem and Information Technology, Chinese Academy of Sciences, 865 Changning Road, Shanghai 200050, People's Republic of China

E-mail: jccao@mail.sim.ac.cn

Received 6 March 2008, in final form 7 May 2008
Published 27 May 2008
Online at stacks.iop.org/JPhysCM/20/255244

Abstract
We study, in single quantum dot (QD) luminescence, the temperature-dependent broadening mechanism due to the coupling between localized excitons and acoustic phonons as well as the environment surrounding the QD system. As a treatment of the interaction between the QD system and the environment, a configuration of excitonic eigenenergies is introduced. Using the Green's function method, analytical formulae of the lineshape of zero-phonon lines (ZPL) are given. The numerical results show that phonons inducing initial fast decay contributes to the background wings of the spectra leading to a wings-asymmetry photoluminescence (PL) spectra. Our model gives a semiquantitative description of the underlying broadening mechanism and is helpful in understanding the origin of the experimental results for the temperature dependence of the ZPL in self-assembled QDs.

1. Introduction

Semiconductor quantum dots (QDs), so-called artificial atoms, have attracted considerable interest as mesoscopic model systems and prospective building blocks of the 'quantum computer'. The interaction between excitons and phonons in semiconductor quantum dots determines the temperature dependence of the optical response and contributes to the dephasing of the optically excited quantum states of the dots. These optical properties are of current interest in connection with the proposed use of quantum dots in implementations of quantum computing.

At low temperatures the photoluminescence (PL) spectra of single dots have a sharp central feature and a broad background [1–5]. The problem of phonon effects on the optical spectra associated with bound electronic states in a crystal was first treated in the context of the spectra of impurities [6–8] and bound excitons in bulk semiconductors [9]. In terms of a perturbation treatment of the electron–acoustic phonon interaction, the central peak in the spectrum is associated with the term involving no phonons and commonly referred to as the zero-phonon line (ZPL). It is an optical analog of the Mössbauer line in the impurity nuclei transitions [9]. This phenomenon was experimentally observed in many single-dot studies. Besides the photoluminescence experiments, time-resolved spectroscopy is employed to study the polarization decay, i.e. the dephasing time which is related to the inverse of the ZPL width [2, 10]. Simultaneous measurements of the dephasing and the population decay for localized excitons in narrow GaAs quantum wells (QWs) show that the elastic interaction with acoustic phonons contributes to dephasing [11] with increasing temperature. Such phase decoherence is called pure dephasing. Generally, for a phenomenological treatment, pure dephasing corresponds to the so-called Markovian process for the elastic exciton–phonon (ex–ph) interaction [13].

The experimentally observed lineshapes have a linewidth that was found to increase linearly with temperature at $T < 50$ K in many single-dot studies [1–4]. In recent four-wave mixing experiments on arrays of dots, the temperature dependence of the linewidth was found to be of an exponential activated form rather than linear [14, 15]. Two different mechanisms involving off-diagonal transitions between quantum dot electronic states have been proposed to explain the ZPL broadening, real transitions from ground to excited states in larger dots [16] and virtual transitions giving higher-order terms in ex–ph interactions [17].

In this paper, in order to explain the observed increasing FWHM (full width at half-maximum) with increasing temperature, we introduce an additional phenomenological phase damping linearly proportional to time [11] and a linear coupling of excitons and phonons as a treatment of the interactions in the broadened system. Theoretically, an independent boson model [18, 19] has often been used for the ex–ph interaction, and it is sufficient to describe the phonon wings' background phenomenon in general quantum dots and the satellite peaks in the optical absorption of nanowire-based quantum dots [20]. On the other hand, to explain the ZPL broadening, several delicate approaches have been pursued in which quadratic couplings to phonons [21–24] and phonon linewidths have been introduced [5, 25]. However, the temperature-dependent lineshape due to the inhomogeneously broadening effect, e.g. exciton density distribution, has not yet been discussed, the origin of which may lead to the power broadening [26, 27] in the luminescence. Except for the ex–ph interaction, many other scatterings contribute to the ZPL, e.g. (i) scattering with elastic and inelastic exciton–exciton (ex–ex) and exciton–electron (ex–e) scattering, etc, and (ii) scattering at impurities and other lattice defects. For a phenomenological description of such an inhomogeneously broadening effect, we assume that the exciton has a slightly different eigenenergy distributed over an interval γ_0 due to coupling to some 'bath' [11, 12]. Consequently we obtain the FWHM which explains the origin of the very different experimental results for the temperature dependence of the ZPL in self-assembled QDs and the emission spectra which show a small asymmetry rather than a symmetric Lorentzian line at high temperature.

2. Theory and calculation

To describe the QDs system, we consider the interactions between a single exciton and acoustic phonons. Due to the influence of the circumstance of the QDs system as in the statement of the previous section, the exciton retarded Green's function can be given by

$$G^{(0)}(t) = \langle B(t)B^{\dagger}(0)\rangle = -\mathrm{i}\exp(-\mathrm{i}\omega_0 t - \gamma_0 t), \qquad t > 0, \tag{1}$$

where $B^{\dagger}(B)$ is the creation (annihilation) operators of the ground state exciton and ω_0 is the center frequency of the exciton. Our assumption is similar to [5] and [25] where finite phonon lifetime is introduced as a treatment of the influence of the interface roughness. We describe the ex–ph interaction under the independent boson model and the general interaction Hamiltonian for a coupled ex–ph system is written as

$$B^{\dagger}B_q M_q(a_q^{\dagger} + a_q), \tag{2}$$

where $a_q^{\dagger}(a_q)$ and M_q are the creation (annihilation) operators of the phonon with momentum q and the matrix element, respectively. Following [25], the first-order approximate solution using the method of linked cluster expansion is employed in the derivation of the exciton Green's function and the general Feynman diagram is shown in figure 1(a),

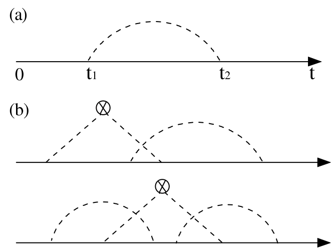

Figure 1. The Feynman diagram for the interaction between the damping exciton and the acoustic phonons. In (a), the solid line and the dashed curve represent the damping exciton Green's function and the free phonon Green's function, respectively. In (b), the solid line, the dashed curve and the cross with a few dashed lines represent the free exciton Green's function, the free phonon Green's function and other scatterings, respectively.

where the solid line and the dashed curve represent a damping exciton Green's function and a free phonon Green's function, respectively. It is sufficient to describe the multiple-phonon effects once the method of linked cluster expansion is used. The involvement of the factor $\exp(-\gamma_0 t)$ in equation (1) describes a mixed effect of ex–ph interactions and other scatterings. However, the cross effects, the Feynman diagrams of which are shown in figure 1(b), are not included in the linked cluster expansion.

Based on figure 1(a), the first-order term in the linked cluster expansion and the exciton retarded Green's function is given by [19]

$$W_1(t) = -\sum_q |M_q|^2 \int_0^t \mathrm{d}t_1 \int_0^t \mathrm{d}t_2 D(q, t_1 - t_2) G^{(0)}(t),$$
$$G^{(1)}(t) = G^{(0)}(t)\exp[W_1(t)G^{(0)}(t)], \qquad t > 0, \tag{3}$$

where $D(q,t)$ is the phonon Green's function. The results in [25] could be generalized once phonon damping effects are included in the expression of $D(q,t)$:

$$D(q,t) = -\mathrm{i}[(n_q+1)\exp(-\mathrm{i}\omega_q t - \gamma_q t) + n_q \exp(\mathrm{i}\omega_q t - \gamma_q t)], \qquad t > 0, \tag{4}$$

where γ_q is the inverse of the phonon lifetime and $n_q = [\exp(\hbar\omega_q/k_B T) - 1]^{-1}$. In a similar way, we employ the Green's function $G^{(0)}(t)$. Then the main result of this paper is given by

$$f(t) = W_1(t)G^{(0)}(t) = -\frac{1 - \mathrm{e}^{-\mathrm{i}\omega_q t} - \mathrm{i}\omega_q t}{\omega_q^2}(n_q+1) - \frac{1 - \mathrm{e}^{\mathrm{i}\omega_q t} + \mathrm{i}\omega_q t}{\omega_q^2} n_q. \tag{5}$$

The spectral function corresponding to the Fourier transform of $G^{(1)}(t)$ could be pursued trivially. Nevertheless the overall lineshape can be deduced by considering the short- and long-time limit of $f(t)$. At short times

$$f(t) \to -\gamma_1^2 t^2, \tag{6}$$

where $\gamma_1 = [\sum_q \frac{1}{2} M_q^2 (2n_q + 1)]^{\frac{1}{2}}$, while at long times

$$f(t) \to -S + \mathrm{i}\Delta t, \tag{7}$$

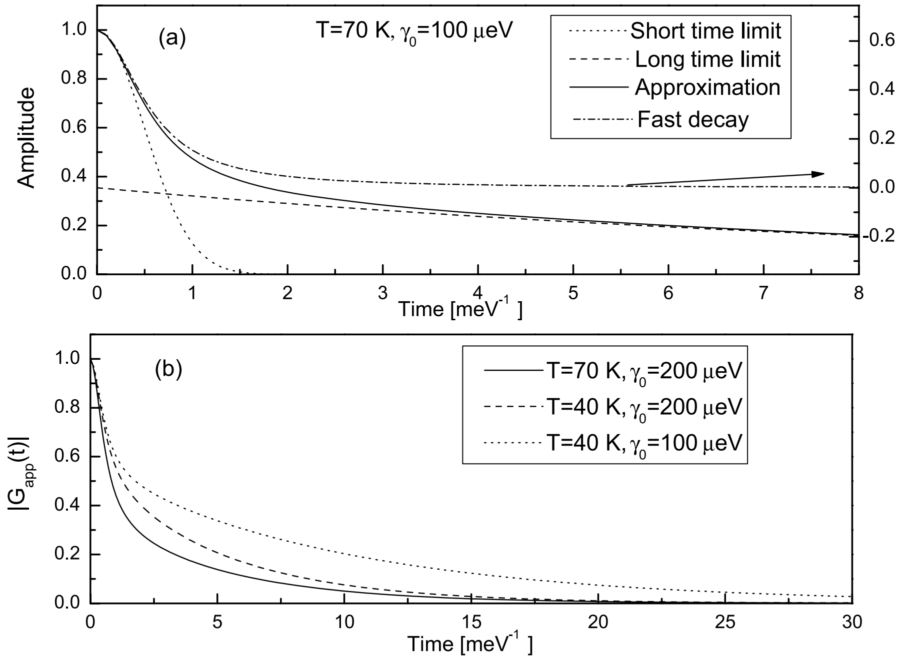

Figure 2. The time-dependent amplitudes calculated for a flat disc-shaped CdTe/ZnTe quantum dot with a radius of 4 nm at several typical temperatures and γ_0.

where the terms which do not contribute to the ZPL width are neglected [25] and the Huang–Rhys factor S and the energy shift Δ are reduced to $\sum_q \frac{M_q^2}{\omega_q^2}(2n_q + 1)$ and $\sum_q \frac{M_q^2}{\omega_q}$, respectively. Usually the γ_1 is large enough and phonon scattering adds a Gaussian broadened background to the spectral function corresponding to the short-time response of equation (3). The long-time response corresponds to a Lorentzian lineshape with a renormalization factor $Z[Z = \exp(-S)]$.

To analyze the overall time response in further detail we evaluate a exponential-power decay [28] to fit the $G^{(1)}(t)$ considering both the short- and long-time behavior. The competent fitting function is given by

$$G^{(1)}(t) \sim G_{\mathrm{app}}(t) = Z\exp(-r_0 t + \mathrm{i}\Delta t) + (1-Z)\frac{1}{1+\gamma_1^2 t^2/(1-Z) - Z(\gamma_0 - \mathrm{i}\Delta)t/(1-Z)}. \quad (8)$$

$G^{(1)}(t)$ is approximately expanded to two terms, the long-time limit and fast decay, where Z and $1 - Z$ correspond to the contributions of the two, respectively. We then deduce the temperature-dependent amplitude, $A(T)$, and FWHM, FWHM (T), by Fourier transforming the approximate function $G_{\mathrm{app}}(t)$:

$$A(T) = \frac{Z}{\gamma_0} + \frac{\pi(1-Z)^{3/2}}{\gamma_1}\exp(-\Delta\sqrt{1-Z}/\gamma_1), \quad (9)$$

$$\mathrm{FWHM}(T) = 2\gamma_0\sqrt{1+\left[\frac{\gamma_1 Z\exp(\Delta\sqrt{1-Z}/\gamma_1)}{2\pi\gamma_0(1-Z)^{3/2}} - \frac{1}{2}\right]^{-1}}, \quad (10)$$

where the temperature dependence enters through γ_1 and Z. Obviously, the damping effect and ex–ph interaction are not coupling in equation (9) and $A(T)$ is also a sum of two terms, the contribution of the long-time limit and the contribution of the fast decay. But the mixed effects enter into FWHM through the second term of the radicand in equation (10).

Table 1. Parameters used in the evaluation of the matrix element M_q. m_e^* and m_h^* are the electron and hole effective mass, D_c and D_v are the deformation potentials of the conduction and valence band, ρ is the mass density, u_s is the angular averaged sound velocity of the longitudinal acoustic phonon mode, Θ_D is the Debye temperature and λ_0 is the in-plane electron–hole correlation parameter.

m_e^*	m_h^*	D_c (eV)	D_v (eV)	ρ (g cm^{-3})	u_s (m s^{-1})	Θ_D (K)	λ_0 (Å)
0.095	0.82	−5.0	1.0	5.51	4.0×10^3	158	42

3. Results and discussion

The only remaining problem for the phonon contribution is to calculate the matrix elements M_q. We consider a flat disc-shaped CdTe/ZnTe quantum dot with a radius of 4 nm. Since the elastic properties of the dot and matrix material are not much different, we neglect its anisotropic dispersion relation and use a 3D phonon model. The material parameters used in the evaluation are shown in table 1 [3].

The time-dependent amplitudes are shown in figure 2 at several typical temperatures and γ_0. In figure 2(a), we plot the long-time limit, short-time limit and $|G_{\mathrm{app}}(t)|$, as well as the fast decay term (the second term of equation (8)). With time developing, $|G_{\mathrm{app}}(t)|$ behaves as a attenuated Gaussian decay in the initial process, decreases more mildly next and, after a few picoseconds, increases to a exponential decay. The approximate function $G_{\mathrm{app}}(t)$ reduces much more

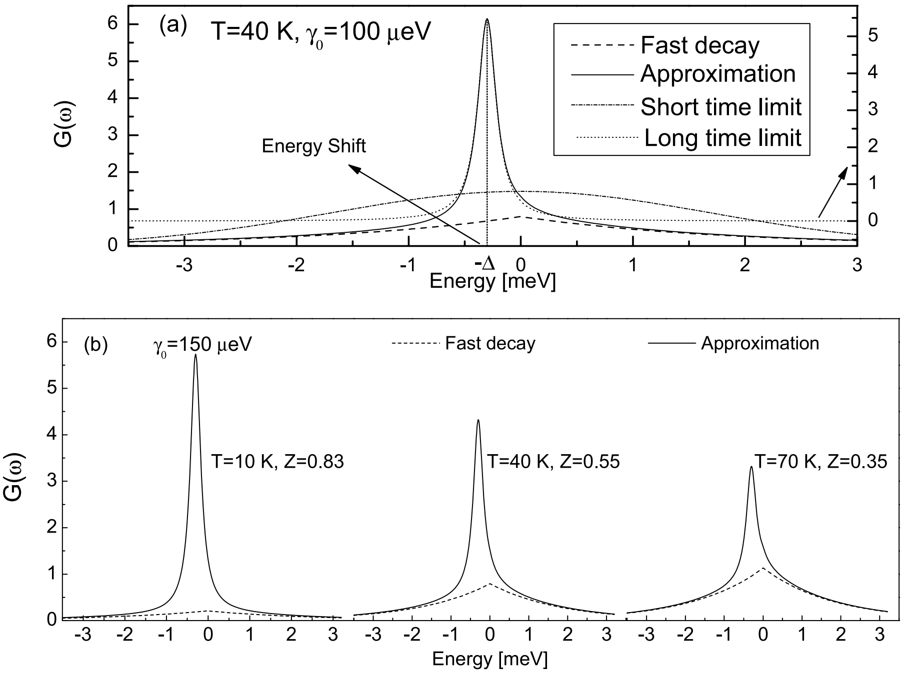

Figure 3. (a) The contrasts between the spectrum functions for the exciton Green's function (solid curves) and the contributions of the fast decay (dashed curves), short-time (dashed–dotted curves) and long-time (dotted curves) limits at $T = 40$ K and $\gamma_0 = 100$ μeV. (b) The temperature-dependent wing-asymmetries at $\gamma_0 = 150$ μeV and the corresponding renormalization factors Z.

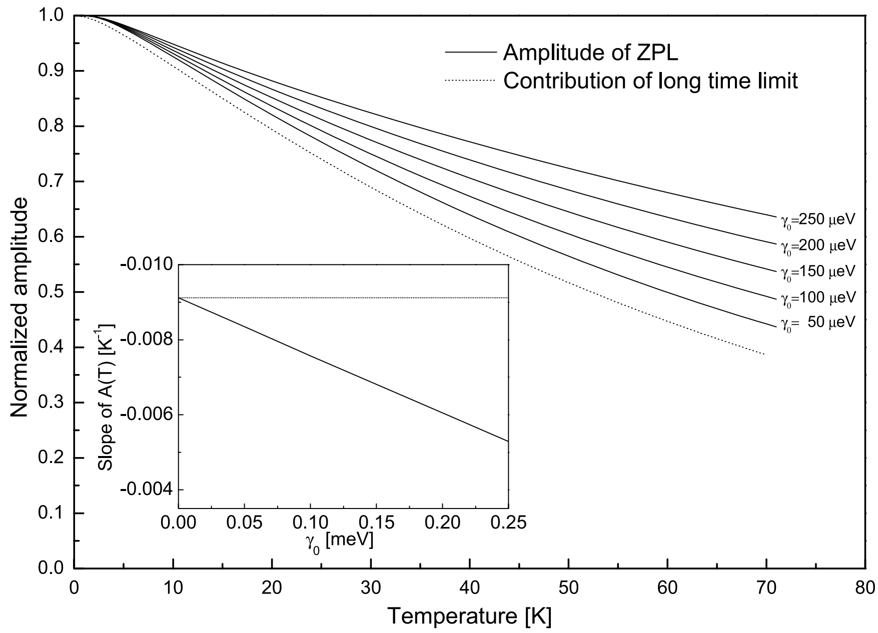

Figure 4. The normalized amplitude of the ZPL (solid curves) at five typical γ_0 (50, 100, 150, 200 and 250 μeV) and the contribution of the long-time limit (dotted curve). The inset illustrates the γ_0-dependent slope.

gently within an initial fast damping time $\sim\frac{\hbar}{\gamma_1}$ than the limit behavior $\exp(-\gamma_1^2 t^2)$. Such a behavior corresponds to plump background wings beside the ZPL. In figure 2(b), $|G_{\mathrm{app}}(t)|$ is plotted at three pairs of data for comparison. The temperature and γ_0 dependence shows that increasing γ_0 leads to the enhancement of the ex–ph coupling.

The optical spectrum is given by the imaginary part of the Fourier transform of $G(t)$. It is composed of background wings and a Lorentzian line with a peak shift Δ leading to a small asymmetry in the high energy edge, as shown in figure 3(a). Furthermore, the asymmetry depends on the renormalization factor Z which decreases with increasing temperature as shown in figure 3(b).

In figure 4, we find that the amplitude of the ZPL is almost determined by the contribution of the long-time limit at low temperature and is nearly linearly decreasing with increasing

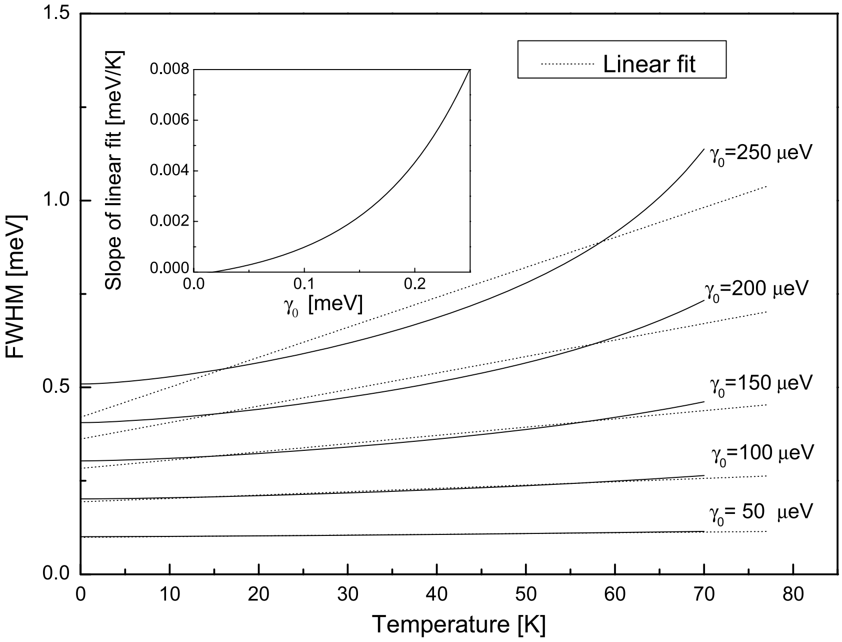

Figure 5. The temperature-dependent FWHM (solid curves) and the lines (dotted lines) at five typical γ_0, and the γ_0-dependent slope of the fitting line (inset).

temperature. The inset of figure 4 shows the linear γ_0 dependence, which could be deduced from the normalization of $A(T)$.

Figure 5 shows the FWHM(T) at five typical γ_0. At $T = 0$ K, the phonons contribute less than 1% to the FWHM and FWHM(0) $\approx 2\gamma_0$. With increasing temperature, FWHM seems to increase as a linear function of the temperature, FWHM(T) − FWHM(0) $= \alpha T$. The linear coefficient α has been evaluated by a linear fit, which is illustrated in the inset of figure 5. At high temperature, the curves have distinct divergence from the fitting lines especially at large γ_0 and approach an exponential activated form instead [29]. The temperature-dependent broadening has entirely profited from the involvement of the second term of equation (8), the corresponding spectrum function of which is illustrated as a dashed line in figure 3(b).

To make our model more understandable, we also calculate the matrix elements M_q for optical phonons. Below $T = 70$ K, the temperature dependence of the lineshape is insensitive to the coupling between optical phonons and excitons for the factor $2n_q + 1 \approx 1$. Thus, the optical phonons just make an additional and temperature-independent contribution to the lineshape. We evaluate Z for the polar coupling between optical phonons and excitons and obtain $Z > 0.95$. The minimum of Z is at $T = 70$ K and even larger values are obtained for the deformation potential coupling. Therefore, the renormalization factor Z approaches unity and is nearly temperature-independent. For these reasons, we have ignored the effect of coupling between optical phonons and excitons. Furthermore, numerical results indicate that optical phonons contribute only a few μeV to the total FWHM. Such effects may be considered as a small portion of the inhomogeneous broadening. Taking account of the localization of the exciton so as to ignore the lattice defects, it can be seen that ex–ex and ex–e scatterings could be the main issue for the inhomogeneous broadening effect.

Comparing our results with the experiments on single dots, the linear coefficient α is indeed smaller than that reported in [3] for the QD, and [30] and [31] for a 18 Å CdTe/$Cd_{0.82}Zn_{0.18}Te$ QW. Such divergence could be due to the neglect of the finite lifetime of phonons. However, the same order (up to 50%) of the linear coefficient α is obtained in our model, which indicates the importance of the coupling of the inhomogeneous broadened effect and the acoustic phonons scattering in single quantum dot luminescence.

4. Conclusions

Except for ex–ph interaction, many other scatterings could influence the optical properties of excitons. Such an inhomogeneous broadening effect is employed to obtain the temperature-dependent FWHM in an ex–ph interactive QD system. Using the Green's function method, the emission spectrum is obtained by introducing a phenomenological and experimentally determined parameter γ_0 and exhibits a small wing-asymmetry, linear temperature-dependent amplitude reduction and FWHM increase. Comparing the experimental data [3] and the previous theoretical results [25], we indicate the importance of the coupling of the inhomogeneous broadened effect and acoustic phonon scattering in single quantum dot luminescence.

Acknowledgments

This work is supported by the National Fund for Distinguished Young Scholars of China (60425415), the National Basic Research Program of China (2007CB310420), the National

Science Foundation of China (60721004) and the Shanghai Municipal Commission of Science and Technology, China (06DJ14008 and 06CA07001).

References

[1] Bayer M and Forchel A 2002 *Phys. Rev.* B **65** 041308(R)
[2] Birkedal D, Leosson K and Hvam J M 2001 *Phys. Rev. Lett.* **87** 227401
Birkedal D, Leosson K and Hvam J M 2002 *Phys. Scr.* T **101** 143
[3] Besombes L, Kheng K, Marsal L and Mariette H 2001 *Phys. Rev.* B **63** 155307
[4] Kammerer C, Voisin C, Cassabois G, Delalande C, Roussignol Ph, Klopf F, Reithmaier J P, Forchel A and Géard J M 2002 *Phys. Rev.* B **66** 041306(R)
[5] Ortner G, Yakovlev D R and Bayer M 2004 *Phys. Rev.* B **70** 201301(R)
[6] Pekar S I 1950 *Zh. Eksp. Teor. Fiz.* **20** 519
[7] Huang K and Rhys A 1950 *Proc. R. Soc.* **204** 406
[8] Krivoglaz M A 1964 *Sov. Phys.—Solid State* **6** 1340
[9] Duke C B and Mahan G D 1965 *Phys. Rev.* **139** A1965
[10] Borri P, Langbein W, Schneider S, Woggon U, Sellin R L, Ouyang D and Bimberg D 2001 *Phys. Rev. Lett.* **87** 157401
[11] Fan X, Takagahara T, Cunningham J E and Wang H 1998 *Solid State Commun.* **108** 857
[12] Gindele F, Hild K, Langbein W and Woggon U 1999 *Phys. Rev.* B **60** R2157
[13] Li X-Q and Arakawa Y 1999 *Phys. Rev.* B **60** 1915
[14] Langbein W, Borri P, Woggon U, Stavarache V, Reuter D and Wieck A D 2004 *Phys. Rev.* B **69** 161301(R)
[15] Borri P, Langbein W, Woggon U, Stavarache V, Reuter D and Wieck A D 2005 *Phys. Rev.* B **71** 115328
[16] Takagahara T 1999 *Phys. Rev.* B **60** 2638
[17] Muljarov E A and Zimmermann R 2004 *Phys. Rev. Lett.* **93** 237401
[18] Vagov A, Axt V M and Kuhn T 2003 *Phys. Rev.* B **67** 115338
[19] Mahan G 1990 *Many-Particle Physics* 2nd edn (New York: Plenum)
[20] Lindwall G, Wacker A, Weber C and Knorr A 2007 *Phys. Rev. Lett.* **99** 087401
[21] Uskov A V, Jauho A P, Tromborg B, Mork J and Lang R 2000 *Phys. Rev. Lett.* **85** 1516
[22] Goupalov S V, Suris R A, Lavallard P and Citrin D 2002 *IEEE J. Sel. Top. Quantum Electron.* **9** 1009
[23] Hizhniyakov V, Kaasik H and Sildos I 2002 *Phys. Status Solidi* b **234** 644
[24] Muljarov E A and Zimmermann R 2004 *Phys. Rev. Lett.* **93** 237401
[25] Rudin S, Reinecke T L and Bayer M 2006 *Phys. Rev.* B **74** 161305(R)
[26] Kammerer C, Cassabois G, Voisin C, Delalande C, Roussignol Ph, Lemaître A and Géard J M 2001 *Phys. Rev.* B **65** 033313
[27] Stufler S, Ester P, Zrenner A and Bichler M 2004 *Appl. Phys. Lett.* **85** 4202
[28] Birkedal D, Leosson K and Hvam J M 2001 *Phys. Rev. Lett.* **87** 227401
[29] Borri P, Langbein W, Woggon U, Schwab M, Bayer M, Fafard S, Wasilewski Z and Hawrylak P 2003 *Phys. Rev. Lett.* **91** 267401
[30] Mayer E J, Pelekanos N T, Kuhl J, Magnea N and Mariette H 1995 *Phys. Rev.* B **51** 17263
[31] Seufert J, Weigand R, Bacher G, Kümmell T, Forchel A, Leonardi K and Hommel D 2000 *Appl. Phys. Lett.* **76** 1872